Rakeness-based compressed sensing of atrial electrograms for the diagnosis of atrial fibrillation

Samprajani Rout*, Mauro Mangia†, Fabio Pareschi¶†, Gianluca Setti¶†, Riccardo Rovatti‡†, Wouter A. Serdijn*
*Section Bioelectronics, Delft University of Technology, The Netherlands;
†ARCES - University of Bologna, Italy; ¶DET - Politecnico di Torino, Italy;
‡DEI - University of Bologna, Italy

***Abstract*—Atrial electrogram (AEG) acquired with a high spatio-temporal resolution is a promising approach for early detection of atrial fibrillation. Due to the high data rate, transmission of AEG signals requires considerable energy, making its adoption a challenge for low-power wireless devices. In this paper, we investigate the feasibility of using compressed sensing (CS) for the acquisition of AEGs while reducing redundant data without losing information. We apply two CS approaches, standard CS and rakeness-based CS (rak-CS) on real medical recordings. We find that the AEGs are compressible in time, and, more interestingly, in the spatial domain. The performance of rak-CS is better than standard CS, especially at higher compression ratios (CR), both during sinus rhythm (SR) and atrial fibrillation (AF). More specifically, the difference in the achieved average reconstruction signal-to-noise (ARSNR) in rak-CS and standard CS, for CR = 4.26, in the time domain is 7.7 dB and 2.6 dB for AF and SR, respectively. Multi-channel data is modeled as a multiple-measurement-vector problem and a suitable mixed norm is used to exploit the group structure of the signals in the spatial domain to obtain improved reconstruction performance over l_1 norm minimization. Using the mixed-norm recovery approach, for CR = 4.26, the difference in achieved ARSNR performance between rak-CS and standard CS is 5 dB and 2 dB for AF and SR, respectively.**

I. Introduction

Atrial electrograms (AEG) are a class of signals that are recorded on the surface of the heart. In addition to electrocardiogram (ECG), which is recorded on the surface of the human body, AEG has the potential to offer deeper insights into the signal propagation in the heart, specifically in the atria, located in its upper part. Worth stressing that AEGs can be used to study the progression of cardiac abnormal conditions such as atrial fibrillation (AF). Irregular R-R intervals [1] and the absence of P-waves characterize AF in an ECG recording. Although characterization of AF in AEGs is not straightforward, it is usually identified with irregular and rapidly varying signals, and appear highly chaotic. The phenomena governing the propagation of the wavefront during AF is poorly understood and the current understanding is limited due to the lack of efficient high-resolution mapping systems [2], [3].

In comparison to recording ECG signals, AEGs are acquired with a high resolution multi-electrode two-dimensional array, which requires continuous acquisition, storage, as well as transmission of a large amount of data. Due to the data-intensive nature of the acquisition of AEGs, developing portable devices for continuous monitoring in the clinical setting is challenging. In particular, for the early diagnosis of AF and understanding of the complex spatio-temporal behavior of the signals recorded on the surface of the heart, both during sinus rhythm (SR) and atrial fibrillation (AF), there is a need for a high-resolution data acquisition system. Yet, the acquisition and transmission of high-resolution data poses a constraint on the power consumption.

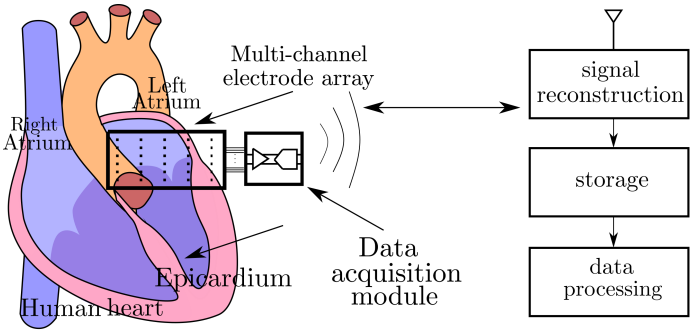

Fig. 1: System-level diagram of the acquisition of atrial electrograms.

A system-level diagram of the acquisition of the AEGs is shown in Figure 1, where the signals are recorded using an integrated array and a recording module, and transmitted to a base station for further processing. With a minimum interelectrode distance of 2 mm, at least 1728 recording sites are required to cover the entire atrium which includes the right atrium, the left atrium and the Bachmann's bundle [4]. For recording signals from 1728 electrodes, at a resolution of 16 bits and a sampling frequency of 10 kHz, the total data rate required is $16 \times 10 \times 10^3 \times 1728$, or 276 Mbit/s, resulting in $\approx$ 16.6 Gbit/min. To acquire and process such a large amount of data for a portable device is a practical challenge due to the needed power and memory requirements.

One of the innovative points of our work is to investigate the compressibility of a new class of signals, i.e., AEGs, both in time and spatial domain. Compressed sensing (CS) is a relatively recent paradigm that allows simultaneous acquisition and compression of a signal by means of sampling it below the Nyquist rate. In the state-of-the-art literature, CS has been successfully applied to various bio-signals, such as ECG, EMG, and EEG [5]–[8], thanks to the property of these signals to be inherently *sparse* in a certain domain. In details, we will investigate the sparsity properties of the AEG signal and com-

978-1-7281-0397-6/19/$31.00 ©2019 IEEE

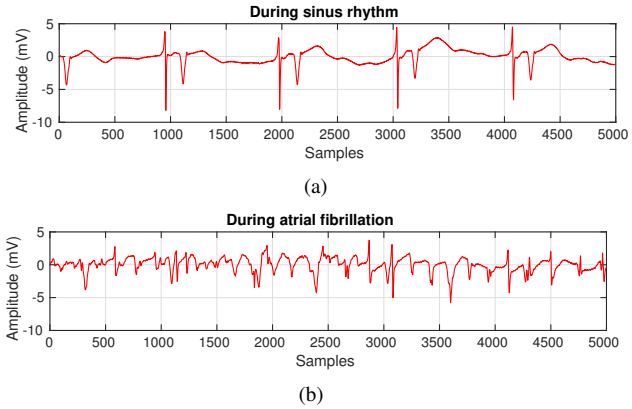

Fig. 2: Time-domain waveform: (a) Normal sinus rhythm (b) Atrial fibrillation (Data courtesy: Erasmus MC, Rotterdam).

pute the expected CS performance with varying compression ratios. We will focus both on single-channel compression in the temporal domain and on multi-channel compression by exploiting the expected similarity among the signals coming from adjacent leads. In Section II, the compressed sensing approach for a single channel and multi-channel AEG signals is explained. In Section III, the performance evaluation of the proposed approach is described. Finally, the conclusions are summarized in Section IV.

II. Compressed Sensing

A. Single channel compressed sensing

Compressed sensing is a method for efficiently sampling signals that are known to be sparse in some basis [9], [10] without loss of information. Exploiting CS significant energy saving can be obtained in acquisition [7] [6], with the further advantage to ensure a certain degree of data privacy [11] [12].

More rigorously, let x be an N-dimensional input vector representing the signal recorded from a single electrode, which is K-*sparse* in a suitable basis $\Psi = [\psi_1, \psi_2 ..., \psi_N]$, $\psi_i \in \mathbb{R}^N$, that is x can be represented as

$$x = \Psi\alpha \tag{1}$$

where α is an N-dimensional vector with only $K \ll N$ non-zero elements in the matrix Ψ. K and N are related by $sparsity$ which is given by $(1 - K/N) \times 100\%$.

Such a sparse vector can acquired by a simple linear combination via a sensing matrix $\Phi = [\phi_1, \phi_2 ..., \phi_M]^t$, $\phi_i \in \mathbb{R}^M$, where $\cdot^t$ denotes transposition, so that the (compressed) measurement vector y can be written as

$$y = \Phi x + n \tag{2}$$

where $y \in \mathbb{R}^M$, $\Phi \in \mathbb{R}^{M \times N}$, $x \in \mathbb{R}^N$and $n \in \mathbb{R}^M$ is the measurement noise, modeled as additive white Gaussian in the temporal domain.

From the compressed measurement samples, the signal can be reconstructed by solving the minimization problem given by

$$\hat{\alpha} = \arg\min_{\alpha} \|\alpha\|_1 \quad \text{subject to} \quad y = \Phi\Psi\alpha \tag{3}$$

where $\|\alpha\|_1$ is the l_1 norm of the signal. Further, the reconstructed input signal is given by $\hat{x} = \Psi\hat{\alpha}$.

The only prerequisite of the standard CS is the sparsity of a signal in an arbitrary basis. However, given a proper class of signals, it is possible to exploit other priors to improve the performance of the CS reconstruction. We focus here on the rakeness-based approach [13], that exploits the input signal energy distribution (i.e, the *localization*). This technique matches the input signal second-order statistics in the design of the measurement matrix. The idea is to increase the average energy of the measurement vector elements (and so, intuitively, the contained information) by a soft adaptation of the statistics of the rows ϕ_j of Φ to the correlation matrix characterizing the class of acquired signals. Mathematically, the rakeness ρ between two processes generating the vectors ϕ_j and x can be defined as [13], [14]

$$\rho(\phi_j, x) = \mathbf{E}_{\phi_j, x}\left[|\langle\phi_j, x\rangle|^2\right] \tag{4}$$

where $\mathbf{E}_{\phi_j,x}$ refers to the expectation with respect both to ϕ_j and x. By selecting a class of matrices Φ that, given x, maximizes ρ there is an observed reduction in the reconstruction error $\|x - \hat{x}\|_2$ after the solution of (3).

B. Multi-channel compressed sensing

Consider a 2-D array of L electrodes where the signal $\mathbf{X}$ is acquired from various channels with a sensing matrix Φ and the measurement matrix $\mathbf{Y}$ can be described as

$$\mathbf{Y} = \Phi\mathbf{X} + \mathbf{n} \tag{5}$$

where $\mathbf{Y} \in \mathbb{R}^{M \times L}$, $\Phi \in \mathbb{R}^{M \times N}$, $\mathbf{X} \in \mathbb{R}^{N \times L}$ and $\mathbf{n} \in \mathbb{R}^{M \times L}$ is the measurement noise, modeled as spatio-temporally white Gaussian noise. Here, $\mathbf{X} = [x_1, x_2, \ldots, x_L]$, where x_j is the signal acquired from the j-th single electrode. Let also $\mathbf{A} = [\alpha_1, \alpha_2, \ldots, \alpha_L]$ the matrix composed by the sparse representation vectors of $[x_1, x_2, \ldots, x_L]$, with $x_j = \Psi\alpha_j$, $j = 1, 2, \ldots L$ or, with a more compact notation, $\mathbf{X} = \Psi\mathbf{A}$.

The multi-channel atrial electrograms share similarities among the adjacent channels, which can be exploited for an improved reconstruction performance. Multi-channel CS acquisition can be formulated as a multiple-measurement-vector (MMV) problem and can be solved with jointly sparse recovery algorithms [15]. The aim of MMV compressed sensing is to recover the jointly sparse $\mathbf{A}$, which can be formulated as [16]

$$\hat{\mathbf{A}} = \arg\min_{\mathbf{A}} \|\mathbf{A}\|_{1,2} \quad \text{subject to} \quad \mathbf{Y} = \Phi\Psi\mathbf{A} \tag{6}$$

where the joint sparsity in $\mathbf{A}$ is induced by the $l_{1,2}$ mixed norm defined by $\|\mathbf{A}\|_{1,2} = \left(\sum_{j=1}^{L}\left(\sum_{i=1}^{N}|\mathbf{A}_{i,j}|\right)^2\right)^{1/2}$.

III. Results

A. Method of data acquisition

Atrial electrograms as shown in Figure 2, are recorded on the epicardium, the surface of the heart, using a custom-made

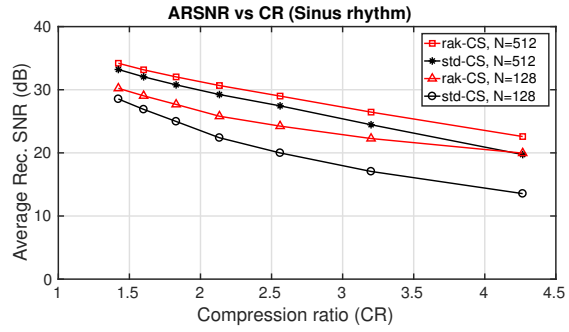

(a)

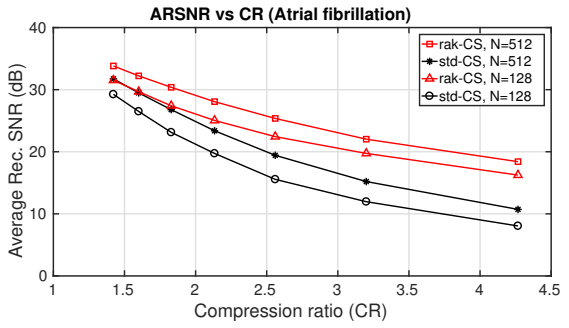

(b)

Fig. 3: Time-domain ARSNR vs CR for the atrial electrograms during: (a) SR (b) AF.

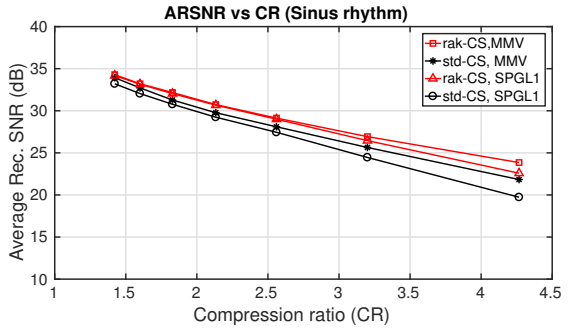

(a)

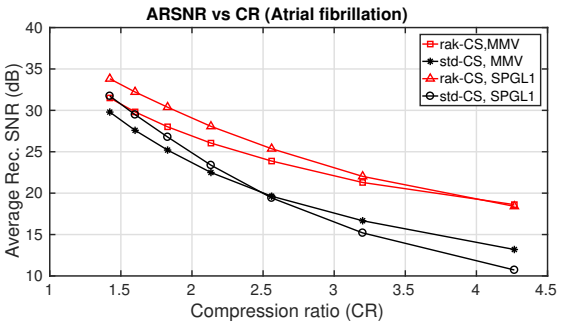

(b)

Fig. 4: Spatial-domain ARSNR using mixed-norm recovery and l_1 norm minimization (for N=512) in case of: (a) SR (b) AF.

46 mm by 14 mm flexible multi-electrode array with 192 gold-plated electrodes and a 256-channel data-acquisition system [4]. The data is acquired using an analog front-end module that consists of an amplifier with a gain of 60 dB, a bandpass filter with the bandwidth extending from 0.5 to 400 Hz and an analog-to-digital converter with a resolution of 16 bits, which samples the analog signal at 1 kHz. A total of 10 electrode array sections are required to cover the entire surface area of the atria. For rak-CS, one of the recorded sections is used as a reference for the correlation matrix estimation. Using the SPGL[1] toolbox, we use the CS decoders to reconstruct the signals by solving (3) and (6), where Ψ is the Symmlet6 transformation basis.

B. Performance evaluation

The reconstructed signal is compared to the original signal using the performance metric, reconstruction signal-to-noise ratio (RSNR) given by

$$\text{RSNR}_{\text{dB}} = 20\log\left(\frac{\|x\|_2}{\|x-\hat{x}\|_2}\right) \tag{7}$$

The RSNR is averaged over all the channels and 9 blocks of the signal for standard and rak-CS in the time domain. Firstly, it can observed that rak-CS performs better than standard CS. The difference in the achieved average reconstruction SNR (ARSNR) performance between the two approaches increases with increase in the compression ratio. In case of SR, at CR

[1]http://www.cs.ubc.ca/∼mpf/spgl1/

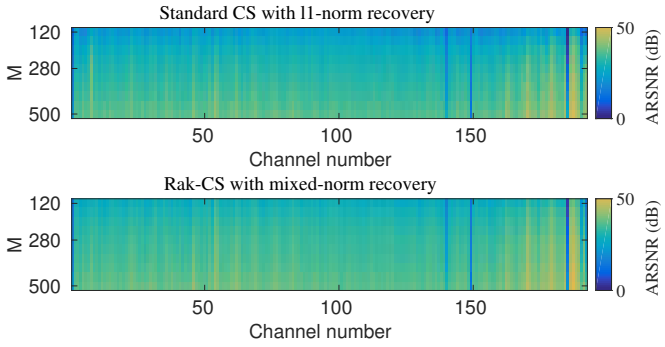

(a)

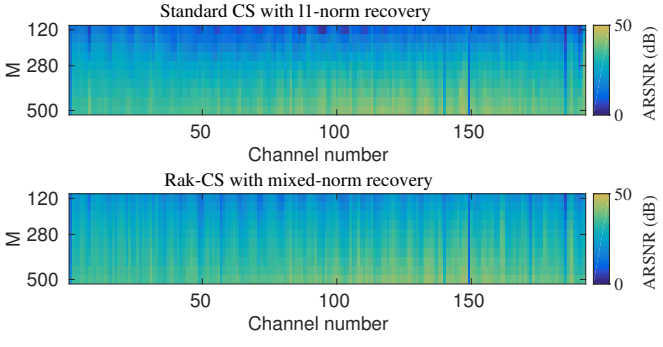

(b)

Fig. 5: ARSNR for 192 channels in case of: (a) SR (b) AF.

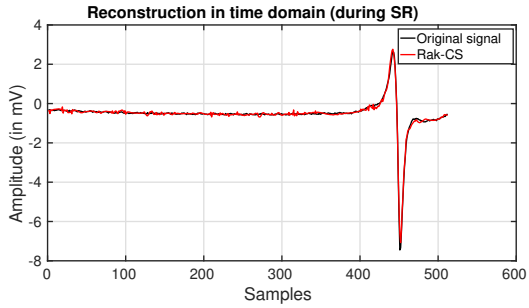

(a)

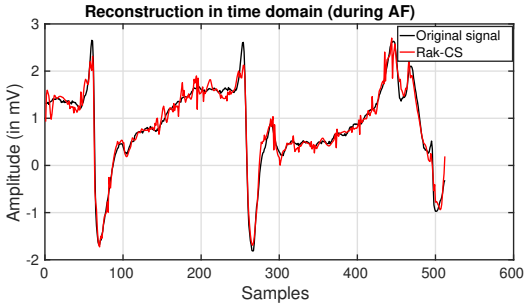

(b)

Fig. 6: Reconstruction of the time-domain waveform of atrial electrograms at CR = 4.26 (N=512): during (a) SR (b) AF.

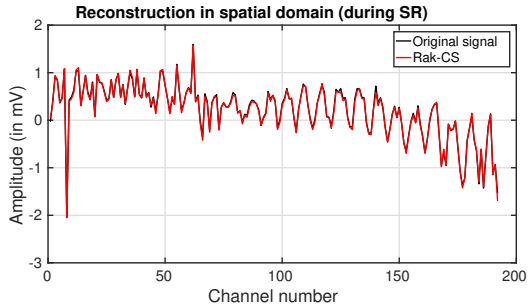

(a)

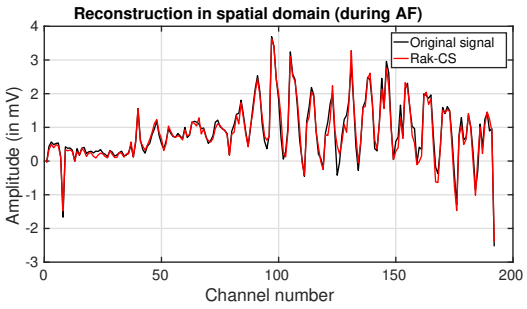

(b)

Fig. 7: Reconstruction of the spatial-domain waveform of atrial electrograms at CR=4.26 (N=512): (a) SR (b) AF.

= 4.26, rak-CS outperforms standard CS by almost 9 dB, as shown in Figure 3(a). In case of atrial fibrillation, at CR = 4.26, rak-CS outperforms standard CS by 7.7 dB, as shown in Figure 3(b). rak-CS accounts for the localization of the signal energy due to which there is a significant improvement in performance at higher CRs (See Section II).

The reconstruction performance of the SPGL1 recovery method which minimizes only the l_1 norm is compared with the mixed norm recovery approach and is as shown in Figures 4(a) and 4(b). It can be seen that the reconstruction performance of the jointly sparse recovery approach is better than independent l_1 minimization recovery and the difference is more pronounced at higher compression ratios. Also, standard CS is compared with rak-CS using the multiple-measurement-vector approach. At CR = 4.26, the ARSNR of the rak-CS approach using the mixed norm recovery is 24.4 dB, which is 4.6 dB better than standard CS with the l_1 norm minimization recovery method, in case of SR.

The ARSNR varies over different channels and compression ratios showing significant differences in the case of SR and AF as shown in Figures 5(a) and 5(b). The fixed dark blue lines on the figures correspond to reference signals. One can observe that the group structure is preserved in case of SR, but the signals are not very similar in case of AF. This points to the fact that during atrial fibrillation, the signals are not coherent and the signal propagation takes place depending on the conduction paths and blocks in the atria.

Figures 6(a) and 6(b) show the reconstruction of the atrial electrograms in the time domain during SR and AF, respectively, for an arbitrarily selected channel number (ch = 90). Figures 7(a) and 7(b) show the reconstruction of the AEGs in the spatial domain, during SR and AF, respectively for an arbitrarily chosen time instant. We can see that the reconstruction of the signal during sinus rhythm is better than during atrial fibrillation for the same compression ratio. i.e, CR = 4.26.

IV. Conclusions

The main findings of the work can be summarized as :

- For the application of AEGs, rak-CS performs better than standard CS at all CRs in both the time domain and the spatial domain.
- At lower CRs, mixed-norm recovery works better in the case of SR since the signals are coherent.
- In the time-domain and the spatial-domain, AF has worse absolute performance compared to SR because of incoherence among signals recorded in different channels and much larger energies involved.
- For the detection of AF, rak-CS is a better choice, as the performance is significantly better than standard CS at higher CRs.

One distinguishing feature of AEGs from other biosignals such as EEG or EMG is the direction of the signal propagation. As the composite cardiac signal propagates in a specific direction, the absence of strong spatial correlations can detect the presence of AF. Finally, the rakeness-based compressed sensing approach holds the potential to reconstruct AF signals with high ARSNR which makes it a strong candidate for the acquisition of AEGs for the detection of AF, especially when aiming for hardware- and power-efficient implementation.

REFERENCES

[1] "IEC-60601-2-25 | Medical electrical equipment - Part 2-25: Particular requirements for the basic safety and essential performance of ambulatory electrocardiographic systems," 2012.

[2] S. P. Lee, L. E. Klinker, L. Ptaszek, J. Work, C. Liu, F. Quivara, C. Webb, C. Dagdeviren, J. A. Wright, J. N. Ruskin, M. Slepian, Y. Huang, M. Mansour, J. A. Rogers, and R. Ghaffari, "Catheter-based systems with integrated stretchable sensors and conductors in cardiac electrophysiology," *Proceedings of the IEEE*, vol. 103, no. 4, pp. 682–689, April 2015.

[3] D. M. van Marion, E. A. Lanters, M. Wiersma, M. A. Allessie, B. B. Brundel, and N. M. de Groot, "Diagnosis and therapy of atrial fibrillation: The past, the present and the future," *Journal of atrial fibrillation*, vol. 8, no. 2, 2015.

[4] A. Yaksh, L. J. van der Does, C. Kik, P. Knops, F. B. Oei, P. C. van de Woestijne, J. A. Bekkers, A. J. Bogers, M. A. Allessie, and N. M. de Groot, "A novel intra-operative, high-resolution atrial mapping approach," *Journal of Interventional Cardiac Electrophysiology*, vol. 44, no. 3, pp. 221–225, 2015.

[5] A. M. Dixon, E. G. Allstot, D. Gangopadhyay, and D. J. Allstot, "Compressed sensing system considerations for ecg and emg wireless biosensors," *IEEE Trans. Biomed. Circuits and Systems*, vol. 6, no. 2, pp. 156–166, 2012.

[6] F. Pareschi, P. Albertini, G. Frattini, M. Mangia, R. Rovatti, and G. Setti, "Hardware-algorithms co-design and implementation of an analog-to-information converter for biosignals based on compressed sensing," *IEEE Trans. Biomed. Circuits and Systems*, vol. 10, no. 1, pp. 149–162, 2016.

[7] D. Gangopadhyay, E. G. Allstot, A. M. Dixon, K. Natarajan, S. Gupta, and D. J. Allstot, "Compressed sensing analog front-end for bio-sensor applications," *IEEE Journal of Solid-State Circuits*, vol. 49, no. 2, pp. 426–438, 2014.

[8] M. Shoaran, M. H. Kamal, C. Pollo, P. Vandergheynst, and A. Schmid, "Compact low-power cortical recording architecture for compressive multichannel data acquisition." *IEEE Trans. Biomed. Circuits and Systems*, vol. 8, no. 6, pp. 857–870, 2014.

[9] E. J. Candes, J. Romberg, and T. Tao, "Robust uncertainty principles: exact signal reconstruction from highly incomplete frequency information," *IEEE Transactions on Information Theory*, vol. 52, no. 2, pp. 489–509, Feb 2006.

[10] D. L. Donoho, "Compressed sensing," *IEEE Transactions on Information Theory*, vol. 52, no. 4, pp. 1289–1306, April 2006.

[11] V. Cambareri, M. Mangia, F. Pareschi, R. Rovatti, and G. Setti, "Low-complexity multiclass encryption by compressed sensing," *IEEE Transactions on Signal Processing*, vol. 63, no. 9, pp. 2183–2195, May 2015.

[12] ——, "On known-plaintext attacks to a compressed sensing-based encryption: A quantitative analysis," *IEEE Transactions on Information Forensics and Security*, vol. 10, no. 10, pp. 2182–2195, Oct 2015.

[13] M. Mangia, R. Rovatti, and G. Setti, "Rakeness in the design of analog-to-information conversion of sparse and localized signals," *IEEE Transactions on Circuits and Systems I: Regular Papers*, vol. 59, no. 5, pp. 1001–1014, 2012.

[14] M. Mangia, F. Pareschi, V. Cambareri, R. Rovatti, and G. Setti, "Rakeness-based design of low-complexity compressed sensing," *IEEE transactions on circuits and systems I: Regular Papers*, vol. 64, no. 5, pp. 1201–1213, 2017.

[15] J. Chen and X. Huo, "Theoretical results on sparse representations of multiple-measurement vectors," *IEEE Transactions on Signal processing*, vol. 54, no. 12, pp. 4634–4643, 2006.

[16] E. van den Berg and M. P. Friedlander, "Theoretical and empirical results for recovery from multiple measurements," *IEEE Transactions on Information Theory*, vol. 56, no. 5, pp. 2516–2527, May 2010.